No. 2995

A NUMERICAL AND EXPERIMENTAL STUDY OF STRATIFIED THERMAL STORAGE

F.J. Oppel A.J. Ghajar, P.E., Ph.D. P.M. Moretti, P.E., Ph.D.

ABSTRACT

A one-dimensional, implicit, finite-difference model of a single stratified thermal storage tank has been developed. The model covers variable flow rates for charging or discharging the thermal storage tank and conduction and turbulent mixing within the water for two different inlet configurations. In order to handle variable flow rates, a "conceptual buffer tank" algorithm was developed. Turbulent mixing occuring in the tank was simulated through thermal eddy conductivity factors, which were determined from experimental data. A decreasing hyperbolic function predicted the best variation of the eddy conductivity factors inside the tank. A general relationship between the inlet eddy conductivity factor and the ratio of Reynolds number over Richardson number was established for the inlets investigated. The simulation model adequately predicted the experimental data. In addition, the model reproduced hydraulic test data better than a recent one-dimensional model found in the literature.

INTRODUCTION

The efficiency of thermal energy systems can usually be improved by providing for thermal storage of hot and cold water. For example, in solar space heating systems, the energy stored during the day can make solar energy available at night for heating. For large air-conditioning systems, utility costs may be reduced by operating the equipment at night, when off-peak electricity rates are low, and using this chilled water that was stored during the night to meet the load demand the next day. With rising utility costs, the promise of dollar savings with storage is encouraging. Yet achieving these savings requires investigating the capability of a storage device to keep the hot and cold fluids from blending.

The design of the device used to store thermal energy is important. The energy placed into this device should be extractable when needed. The simplest model of such a device is the single well-mixed storage tank, but this model does not separate the hot and cold fluids in the tank; therefore, this design recovers only a small portion of available energy.

Another approach is the use of multiple storage tanks. This model can improve on the recoverable energy extracted from the system, yet it doubles the tank capacity and requires the cost and complexity of several tanks and many connections.

A third approach is to use a single tank that uses stratification to separate the hot and cold fluids. Here the hot water with the low density is floated directly on top of the cool water with the higher density, resulting in the advantages of the multiple tank system but with a single tank. The inlet fluid must be placed within the tank with minimal

Fred J. Oppel, graduate student, School of Mechanical and Aerospace Engineering, Oklahoma State University, Stillwater, OK; now with Sandia National Laboratories, Albuquerque, NM. Dr. Afshin J. Ghajar, associate professor, and Dr. Peter M. Moretti, professor, School of Mechanical and Aerospace Engineering, Oklahoma State University, Stillwater, OK.

disturbance of the existing fluid in the tank. The success of this scheme depends upon the design of the inlet; one such design has been demonstrated by Sharp (1978).

Several analytical and empirical models of stratified thermal storage have been developed in the literature, for example, Lavan and Thompson (1977), Cabelli (1977), Sha and Lin (1978), Han and Wu (1978), Sharp (1978), Abdoly (1981), and Cole and Bellinger (1982). Further details are given by Oppel (1985). These models in general do not adequately account for the turbulent mixing occuring in the tank as a function of inlet geometry and pertinent dimensionless physical parameters (i.e., Reynolds number and Richardson number). Consequently, due to underestimation of turbulent mixing in the tank, the temperature profile inside the storage tank was not predicted accurately. In addition, such models do not give an insight on the effect of the inlet design on turbulent mixing.

The aim of this paper is to develop an analytical model that predicts the turbulent mixing occurring inside the tank and obtain a functional relationship for the turbulent mixing inside the tank, represented by an eddy conductivity factor, in terms of pertinent dimensionless physical parameters and the inlet configuration. This relationship will be established based on both published experimental data and our own hydraulic model tests with saline solutions for density stratification, using dye for flow-visualization. Using mixing factors from this analytical model, a computer program can be developed that will predict the temperature profile in the storage tank as a function of time, if the history of inlet flow and temperatures is provided. These profiles will predict the water temperature at the tank outlet. Such a program is not only a testable end product and an enhancement of our stratification simulation capability, but it is also a useful input into a total system simulation project.

PHYSICAL MODEL

The storage geometry modeled is a vertical cylindrical tank. The assumptions on which the model is based are as follows:

1. One-dimensional fluid flow and heat conduction, which means that the thermocline is axisymmetric and independent of the radial distance. Agreement of this assumption with experiments is acknowledged by Sharp (1978).

2. Small losses due to conduction through the walls of the tank, achieved by insulating the tank. This assumption predicts that the changes of the thermocline are dominated by conduction and convection of the fluid instead of conduction through the walls. This is in agreement with the findings of Abdoly (1981) if the tank is insulated to obtain maximum efficiency.

3. The walls of the tank are not overly massive, reducing the tendency of the tank to retain heat within the walls and minimizing conduction of heat down the walls of the tank. This is in agreement with Abdoly (1981).

4. The inlet temperature of the flow is beyond the extremes of the temperatures within the tank. That is, the temperature of fluid flowing in the top of the tank must be at least as hot as the fluid at the top of the tank, and the converse must be true for the cold fluid at the bottom inlet.

The equation governing the stratified thermal model for conduction and convection is the energy equation:

$$\frac{DT}{Dt} = \frac{k}{\rho C_p} \nabla^2 T \qquad (1)$$

where D/Dt is the substantial derivative. Now applying this to one-dimensional flow in the x-direction, which is assumed to be positive upward, Equation 1 reduces to:

$$\frac{\partial T}{\partial t} + V \frac{\partial T}{\partial x} = \alpha \frac{\partial^2 T}{\partial x^2} \qquad (2)$$

Equation 2 can be split into two special cases; namely the conduction case (involving only

mixing with no flow) and the convection case (involving only flow with no mixing). Numerical procedures will be applied to Equation 2 for these two special cases in order to verify the simulated results, since the theoretical results for the two cases are known, as shown in Figures 1 and 2, for the conduction and convection cases, respectively.

Conduction-Only Model

This special case of conduction only depleting the thermocline occurs when the velocity term in Equation 2 is zero. Thus Equation 2 reduces to the following form.

$$\frac{\partial T}{\partial t} = \alpha \frac{\partial^2 T}{\partial x^2} \tag{3}$$

Define $Fo = \alpha \Delta t / \Delta x^2$ (the "finite-difference" Fourier number) and AMIX = (EDDY)(Fo) (nondimensional mixing parameter), where EDDY is the nondimensional eddy conductivity factor. Let EDDY = $(\alpha + \varepsilon)/\alpha$, where ε depends on mixing and is similar to an eddy conductivity. For laminar mixing: $\varepsilon = 0$, EDDY = 1, and AMIX = Fo. The fully implicit finite-difference approximation of Equation 3 is given by Equation 4 below.

$$(-AMIX)T'_s + (1+2\ AMIX)T'_p + (-AMIX)T'_n = T_p \tag{4}$$

where the superscript (prime) represents the temperature at the new time step and the subscripts n,p, and s represent the temperature north or above slab p, the temperature in slab p, and the temperature south or below slab p.

Equation 4 was solved using the TDMA (Tri-Diagonal-Matrix-Algorithm) and predicted the exact form of the theoretical curves shown in Figure 1 for the conduction-only case for any value of AMIX.

Convection-Only Model

The convection model, also known as the flow-only model, involves water flowing through the tank, with no mixing between the water initially in the tank and the incoming water. Thus we obtain perfect stratification in the tank and recover 100 % of the energy put into the tank. The simplified equation for this situation for the one-dimensional case with the conduction term equal to zero in Equation 2 is as follows:

$$\frac{\partial T}{\partial t} + V \frac{\partial T}{\partial x} = 0 \tag{5}$$

To obtain the numerical equation, the upwind differencing technique was used in order to compensate for the directional change of water when flowing either into the top or bottom of the tank (Chow 1983). Solving for the temperature at the new time level and defining $FLOW = V\Delta t/\Delta x$ (also known as the Courant number, Chow 1983) where V is the velocity magnitude, we obtain Equation 6 for water flowing into the top of the tank and Equation 7 for water flowing into the bottom of the tank.

$$T'_p = (FLOW)\ T_n + (1 - FLOW)\ T_p \tag{6}$$

$$T'_p = (FLOW)\ T_s + (1 - FLOW)\ T_p \tag{7}$$

To insure stability of Equations 6 and 7, the FLOW parameter must not be greater than 1. Since the stratified case or convection-only case contains no mixing (i.e., EDDY = 0), the temperature profile should resemble the plot shown in Figure 2. Notice that the temperature of the incoming flow replaces the previous temperature of the slab and continues to march toward the exit of the tank as the time elapses. The equation that would produce the temperature profile for water flowing into the top of the tank, as shown in Figure 2, is given by Equation 8 below.

$$T'_p = T_n \tag{8}$$

When trying to simulate the temperature profile in Figure 2 with Equation 6, we see that the FLOW parameter must be equal to one. The simulated results with FLOW = 1 are the same as

the theoretical results in Figure 2. If FLOW is less than 1, our algorithm produces a temperature profile as shown in Figure 3. Notice that this temperature profile is physically incorrect for the stratified flow case. The situation of FLOW = 1 implies that the incoming flow of water must fill up one slab volume in the tank during the time interval of calculation, Δt. Therefore, if Δt and Δx are fixed values, the velocity of the incoming flow is restricted to $V = \Delta x/\Delta t$ for FLOW = 1. Thus the flow rate must remain constant. If FLOW < 1, then we obtain pseudo-mixing (also known as numerical diffusion or artificial viscosity, Chow 1983), as shown in Figure 3.

To overcome the problem of not being able to vary the flow rate of the incoming flow in the algorithm, two fictitious buffer tanks are placed at the ends of the main tank. The purpose of using the buffer tanks was to allow for a variable flow rate and eliminate the pseudo-mixing in the algorithm when FLOW < 1. The buffer tanks store the incoming flow of water when FLOW < 1 and continue to accumulate the incoming flow of water until the amount of water in the buffer tank is equal to at least one slab volume in the tank, which is the same as FLOW = 1. Then one slab volume of water in the buffer tank is pulsed into the main tank. Numerically this means that the Equations 6 and 7 derived for stratified flow are used only when FLOW = 1, leaving the following equations:

For water flowing into the top of the tank

$$T'_p = T_n \tag{9}$$

For water flowing into the bottom of the tank

$$T'_p = T_s \tag{10}$$

Using the buffer-tank concept, the correct form of the temperature profile for the convection-only case, as shown in Figure 2, can be produced.

Combination of Flow and Conduction

To obtain the combined effect, the methods described above can be added together. The conduction-only routine will be applied at each time interval of calculation, whereas the convection-only routine will be applied only if there is enough backlog so that we can set FLOW = 1. The convection-only routine might be invoked only occasionally, for example, every third or fourth time, depending on the flow rate. Thus we can now simulate a combined condition, without introducing pseudo-mixing through numerical procedures, by executing the flow calculations at variable time intervals that are integral multiples of the minimal times.

COMPUTER PROGRAM DEVELOPMENT AND STABILITY CRITERION

A partial listing of the variables used in the computer program and discussed in this paper is shown in Table 1. The user of the program must input several variables to the program such as: A, H, QMAX, TO, TIN. One of the two variables, DELT or NSLAB, must be input to the program based upon the choice of the user, while the other one will be calculated from the flow stability criterion. The values of the remaining variables listed in Table 1 will be either calculated or chosen by the program.

This program will choose the eddy conductivity factor called EDDY in the program. Since EDDY can vary for each slab in the tank, some flexibility is introduced into the one-dimensional flow model. By selecting certain values of EDDY for different slabs, some of the two-dimensional flow properties can be absorbed into this weighting factor (EDDY) for our one-dimensional flow model.

As mentioned above, DELT or NSLAB will be calculated from the flow stability criterion as stated below in Equation 11, where NSLAB = H/DELX.

$$\text{FLOW} = \text{VEL} * \text{DELT} / \text{DELX} \leq 1.0 \tag{11}$$

Notice that the maximum velocity, VMAX, must be known. VMAX can be calculated from the input value QMAX. DELT or NSLAB can be calculated as follows:

$$DELT \leq H / (NSLAB * VMAX) \quad (12)$$

$$NSLAB \leq H / (VMAX * DELT) \quad (13)$$

Appropriate integer values satisfying Equations 12 and 13 for DELT (calculated from the user-supplied NSLAB) or NSLAB (calculated from the user-supplied DELT) will be used in the program.

Evaluating Boundary Conditions

Since the assumption of a well-insulated tank is used in this work, the temperature gradient across the boundaries, that is, the top and bottom of the tank, is assumed to be zero. Thus a fictitious slab is introduced outside the end walls of the tank. These fictitious slabs have the same properties as their corresponding interior end slabs, as if a mirror image occurred. For the conduction-only case, the boundary conditions at the bottom and top of the tank are given below by Equations 14 and 15, respectively.

$$T'_n = T_p \quad (14)$$

$$T'_s = T_p \quad (15)$$

With these boundary conditions, the order of updating the temperature profile should start where the flow enters and should end at the exit. Therefore, the direction of the incoming flow is important in the conduction routine in order to produce the correct order of updating the temperature. The form of the equation at the boundaries is the same as Equation 4. However, the coefficients in Equation 4, evaluated at the boundaries, change based on the direction of the flow into the tank.

For water flowing into the top of the tank

$$(-AMIX)T'_s + (1 + 2\ AMIX)T'_p = (1 + AMIX)T_p \quad (16)$$

For water flowing into the bottom of the tank

$$(1 + 2\ AMIX)T'_p + (-AMIX)T'_n = (1 + AMIX)T_p \quad (17)$$

The buffer tank concept resolves the difficulty of handling the boundary conditions in the flow routine by using a top and bottom buffer tank. Conservation of mass is also satisfied by this method. For example, when the inlet flow changes from the top to bottom, the amount of water left in the top buffer is retained until water flows into the top buffer again; likewise for the bottom buffer tank. Also note that conservation of energy within the buffer tanks was not considered, since it is assumed that the inlet temperature flowing into the buffer tanks remains constant where the top buffer tank remains hot and bottom buffer tank remains cold. Thus the mixing effects in the buffer tanks will be insignificant due to the constant inlet temperature. Even if the inlet temperature does vary somewhat, the mixing effect occurring inside the buffer tank will be insignificant, since the volume of the buffer tanks is very small compared to the volume of the main tank.

With the development of the numerical equations and the employment of the above boundary conditions, an overall simulation program can be produced. Details on the development of the computer program may be found in Oppel (1985).

SIMULATION RESULTS

Having developed the simulation program in the previous sections, the next step was to verify the model through simulation of the published experimental data (Sharp 1978; Abdoly 1981; Cole and Bellinger 1982). In order to simulate the thermocline inside the tank and establish that turbulent mixing occurs in the tank, the eddy conductivity factor ε in AMIX (nondimensional mixing parameter) should be determined. This requires knowledge of temperature data versus slab locations inside the tank at different times. The experimental data of Sharp (1978) were used for this purpose. The next simulation was performed with experimental data of Abdoly (1981) in order to establish the functional form for variation of the eddy conductivity factor from the inlet to the exit of the tank. Finally, the dependency

of the eddy conductivity factor on the inlet configuration was simulated with experimental data of Cole and Bellinger (1982). The results of these simulations will be presented and discussed next.

Thermocline Simulation Inside the Tank

Simulation of thermocline inside the tank and establishment of the existence of turbulent mixing in the tank was accomplished via experimental data of Sharp (1978), which contain temperature data versus slab locations inside the tank at different times, as shown in Figure 4. The type of experiments shown in this figure consisted of charging the initially cold tank with hot water through the inlet at the top of the tank. Notice that the inlet temperature decreased during the operation of the experiment. The first two curves will be analyzed individually, assuming that the inlet temperature for each curve remains constant. An appropriate eddy conductivity factor, determined from trial and error through simulations, will be chosen for each curve. Thus the variation of the eddy conductivity factor from the inlet to the outlet in the tank may be determined. Only two curves will be simulated (0.5 and 1 h) since the last curve (1.5 h) does not contain the full thermocline.

The data needed and used for input into the computer program are listed in Table 2. The properties used were evaluated at the average temperature, between TO and TIN. The parameter NSLAB was chosen as 20, since there were 20 thermocouple locations inside the tank. With the parameter NSLAB fixed, DELT must be calculated from the stability criterion. DELT must be less than 4.28 minutes for the FLOW criterion, and DELT of 3 minutes was used for ease of comparison with the data. Both curves were simulated for three different cases. The first case contained only laminar conduction with $\varepsilon = 0$, which will show whether turbulent mixing is occurring. The second case considered a uniform eddy conductivity factor throughout the tank. The third case consisted of varying the eddy conductivity factor within four equal regions of the tank. This case was considered in order to see if the eddy conductivity factor varies from the inlet to the outlet. Four equal regions were arbitrarily chosen. Only the graphical results of the second case will be presented in this paper. For the results of the other two cases refer to Oppel, Ghajar, and Moretti (1986) and Oppel (1985).

Simulating the first curve (0.5 h) will help predict the degree of mixing occurring near the inlet. The results of the laminar case did not predict the experimental data accurately, indicating that turbulent mixing is occurring as was expected. Figure 5 shows the uniform turbulent case with an eddy conductivity factor of 20. This simulated profile matches the experimental profile very well and does a better job than the model developed by Sharp (1978). For the varying case, the eddy conductivity factor was chosen to vary from a maximum at the inlet to a minimum at the outlet where no mixing exists. The results of the varying profile was nearly identical to the uniform case. This may be attributed to the fact that the eddy conductivity value near the inlet of the tank for the varying case was almost equal to the uniform eddy conductivity value. Thus the eddy conductivity values at the outlet of the tank essentially have no effect, since the temperatures have not changed yet.

Simulating the second curve (1.0 h), which occurs later in time and further down the tank toward the oulet, will determine how the eddy conductivity value changes with time and distance into the tank. The results of the laminar case for the second curve revealed that a smaller amount of turbulence occurred as the thermocline advanced toward the exit. Again the experimental data were not predicted accurately when mixing was not considered. In Figure 6, a uniform eddy conductivity factor of 10 produced a simulated profile similar to the experimental profile. Therefore, the turbulent eddy conductivity factor has decreased during the movement of the thermocline toward the outlet. Notice that the experimental temperature above the thermocline has decreased due to the variation of the inlet temperature, as indicated by Sharp (1978). If the inlet temperature had remained constant during the experiment, this decrease would not be as noticeable. The results of the varying case again produced results nearly identical to the uniform case. The simulated profiles of both the uniform and varying cases match the experimental profiles, except at the location above the thermocline for the reasoning mentioned above.

In comparing our one-dimensional model with Sharp's (1978) one-dimensional model, as shown in Figures 5 and 6, our model simulated results that consistently lay on or near the thermocline, whereas his one-dimensional model produced a thermocline wider and flatter than the experimental thermocline. This suggests that Sharp's model did not consider enough mixing in the portion of the tank near the inlet. Table 3 summarizes the results of both curves. Observing this table along with the temperature plots, the eddy conductivity factor is shown to vary from a maximum value at the inlet to a minimum value at the outlet as the

thermocline moves from its development at the inlet to its depletion at the exit.

Eddy Conductivity Variation

The previous results indicate that turbulent mixing does occur and that it decreases in some fashion from the inlet to the exit. Therefore, two unknowns still exist: the amount of mixing and how it decreases. In order to eliminate one of the unknowns, the best representative function that predicts the variation of the eddy conductivity factor from inlet to exit should be obtained. Once the proper function is determined, then the only unknown to be determined is the value of the inlet eddy conductivity for that particular function. Knowing this inlet eddy conductivity value and the decreasing function defines the eddy conductivity values throughout the tank.

For this purpose three different decreasing functions (e.g., linear, exponential, and hyperbolic) were used to represent variations of the eddy conductivity factor inside the tank from the inlet to the exit and simulate the experimental data of Abdoly (1981). Abdoly reported outlet temperature versus time for several different flow rates with approximately the same temperature difference between the inlet water and initial water in the tank. His cylindrical test tank contained circular baffle plates at each end, with 561 drilled holes for a total opening area of 0.078 square feet per baffle plate. Using these data, the function that best reproduced the experimental data for all the flow rates was determined to be the decreasing hyperbolic function. This function is given by Equation 18, and its variation from the inlet to the exit is depicted in Figure 7.

$$EDDY = A\left(\frac{1}{ISLAB}\right) + B \tag{18}$$

where

For flow into the bottom:

$$A = \frac{E_{INLET} - 1}{1 - \frac{1}{NSLAB}}$$

$$B = E_{INLET} - A$$

For flow into the top:

$$A = \frac{1 - E_{INLET}}{1 - \frac{1}{NSLAB}}$$

$$B = 1 - A$$

Figure 8 shows typical simulation results and comparison with the experimental data of Abdoly (1981) using the proposed mixing function, Equation 18. For all flow rates, the simulated results agreed very well with the experimental data. Further details on the development of the mixing function and comparison of the simulated results with the experimental data may be found in Oppel (1985). Table 4 summarizes the simulated inlet eddy conductivity factors along with the corresponding experimental data of Abdoly (1981). The characteristic length in the Reynolds number is based on the inside tank diameter. The characteristic length in the Richardson number is based on the effective tank height (i.e., height between inlet and outlet). The velocity in both Reynolds and Richardson numbers is that through the tank (i.e., the ratio of the volumetric flow rate to the tank cross-sectional area).

Inlet Geometry Dependency

In order to determine the dependency of the eddy conductivity factor on inlet geometry, experimental data of Cole and Bellinger (1982) were used. They reported outlet temperature versus time for several different inlets, keeping the flow rate and temperature difference constant. The side inlet-outlet and dual radial diffuser were chosen for this investigation. The simulated results for these two inlets are shown in Figures 9 and 10,

respectively. The side inlet-outlet geometry required twice the amount of eddy conductivity as did the dual radial diffuser for this particular flow rate. This indicates that the eddy conductivity is definitely dependent upon the type of inlet geometry.

The lack of available experimental data for a range of flow rates (Reynolds numbers) and temperature differences (Richardson numbers) for different inlet configurations restricts further investigation concerning the eddy conductivity functional relationship with the inlet geometry. This topic should be investigated in more detail and thus requires more experimental data for different inlets. The next two sections of this paper will present our contribution in this area.

OSU EXPERIMENTATIONS

It was established in the previous section that eddy conductivity is a strong function of the inlet geometry. In order to determine its functional relationship, experimental temperature data for different inlets at different Reynolds and Richardson numbers are required. Abdoly's (1981) experiments (see Table 4) were the only useful set of experiments available for this purpose. Therefore, to complete our analysis it was necessary to produce our own experimental data at different Reynolds and Richardson numbers for a different type of inlet design. A 23.5 gallon plexiglass vertical cylindrical tank with an inside diameter of 11 7/16 inches, height of 52.8 inches, and wall thickness of 1/4 inch was used as the test tank. The inlet geometry contained a vertical inlet impinging on a solid circular baffle plate with a diameter of 11 1/4 inches, leaving an annular space 3/32 inches wide. Metered flows enter the tank by gravity from elevated supply tanks holding water at selected densities. Salt concentration (conductivity) was monitored at the inlet and outlet and within the tank. Dye was injected at various points for flow visualization purposes. The experimental procedure and the complete apparatus are described by Oppel (1985).

Flow visualization revealed that mixing increased as the flow rate increased or the density difference between inlet and initial states decreased. The amount of mixing was more sensitive to the changes in the flow rate than the changes in the density difference.

A total of nine experiments were conducted for various flow rates (Reynolds numbers) and density differences (Richardson numbers). Salt concentration at the inlet, outlet, and several different locations in the tank was recorded by means of a conductivity probe. These measured salt concentrations were converted into equivalent temperatures from similitude. Using data recorded over time, the simulation program determined the amount of turbulent mixing in the tank. Table 5 summarizes the simulated inlet eddy conductivity factors along with the corresponding OSU experimental data. For the inlet eddy conductivity values tabulated in Table 5, excellent agreement between the simulated results and experimental data was achieved for all flow rates. For further detail refer to Oppel (1985).

Stratification using saline solutions has been useful for obtaining a wide range of densities. However, because the Lewis number (ratio of thermal diffusivity to molecular diffusivity) for salt in water is not unity, this technique models thermal effects only if turbulent mixing is the dominant mechanism. Therefore, for very low Reynolds numbers (or very high Richardson numbers), it is necessary to use thermally stratified water. However, we have found that for many stratified-storage flows, turbulent mixing is the predominant mechanism and the turbulent Lewis number approaches unity.

INLET EDDY CONDUCTIVITY RELATIONSHIP

The values of the inlet eddy conductivity factor for the circular baffle inlet of Abdoly (1981) and solid circular plate inlet of this work were determined in the previous sections and are tabulated in Tables 4 and 5, respectively. The next step is to determine the inlet eddy conductivity relationship with Reynolds number and Richardson number for both inlets. Knowing the inlet eddy conductivity factor, the eddy conductivity variation inside the tank from the inlet to the outlet can be calculated from Equation 18.

The relationship between the inlet eddy conductivity factor and the two dimensionless numbers will first be examined for the OSU experimental data. The inlet eddy conductivity

factors can be represented by a straight line when plotted in terms of the ratio of Reynolds number over Richardson number (Re/Ri) on a log-log scale, as shown in Figure 11. All of the nine experimental points at different Re and Ri values lie on or near the straight line. The straight line may be represented by an algebraic expression of the form

$$E_{INLET} = a(Re/Ri)^b \tag{19}$$

where the slope (a) and the intercept (b) could be determined from the least squares fit for the straight line through the data points. For the nine OSU experimental data points from the least squares fit, a = 4700 and b = 0.905.

A functional relationship has been established for the inlet geometry used in this work. The value of the inlet eddy conductivity factor can now be calculated for any given Reynolds number and Richardson number. After obtaining this inlet value, Equation 18 can predict the eddy conductivity variation from the inlet to outlet inside the tank.

In order to test the form of the relationship developed, Abdoly's (1981) inlet eddy conductivity factors were plotted against the ratio Re/Ri, as shown in Figure 12. All five experimental points lie on or near the straight line, just as the OSU experiments did. Therefore, the form of the relationship of Reynolds number to Richardson number is the same for both cases, as shown in Equation 19. A least squares fit produces the two constants a and b for the Abdoly's inlet as a = 2320 and b = 0.176. Only the constants in Equation 19 have changed for the two different inlets.

The obtained results are very encouraging. A general relationship seems to hold for the two different inlets that were investigated. In order to verify the universality of this relationship, more experimental data for different inlets must be obtained.

CONCLUSION

The results show that a very simple numerical model can accurately simulate a stratified storage tank. The only precaution necessary was to separate the conduction and convection algorithms in order to eliminate the gradual "smearing" of the temperature profiles in the convection-only (flow-only) case. The conduction algorithm was applied at each time step, and the convection algorithm was applied whenever the buffer tank contained one slab volume. A variable integer relationship between time steps was achieved by means of conceptual buffer tanks.

Turbulent mixing was included with conduction by introducing an eddy conductivity factor, which decreased from a maximum value at the inlet to a minimum value at the outlet. The decreasing hyperbolic function (mixing function) predicted the best variation of the eddy conductivity factor inside the tank. A general relationship between the inlet eddy conductivity factor and the ratio of Reynolds number over Richardson number was found to exist for two different inlet configurations. Only the two constants, a and b in Equation 19, change for the different inlets.

The simulation model developed, adequately predicted the experimental data found in the literature and our own experimental data. Thus the model is flexible enough to be used for different inlet configurations. Also, the flow visualization experiments helped to verify the mixing trends occurring inside the tank.

This one-dimensional model is efficient enough to be incorporated in simulations of complex chilled-water systems such as a campus-wide air conditioning system. At the same time, it reproduced hydraulic test data better than a recent one-dimensional model found in the literature, because of the care taken with the items mentioned above.

Our continuing efforts include conducting flow visualizations and measurements using dye and either salt solutions or heated water to study inflows and mixing rates in stratified tanks for several styles of inlet configurations and various density ranges and inflow conditions (Richardson and Reynolds numbers), for the purpose of establishing the unversality of the proposed inlet eddy conductivity relationship. Planned research also includes fluctuating inlet temperatures.

NOMENCLATURE

a = multiplication coefficient in inlet eddy conductivity equation, see Equation 19

A = multiplication coefficient in EDDY equation, see Equation 18

AMIX = dimensionless mixing parameter, AMIX=(EDDY)(Fo)

b = exponential coefficient in inlet eddy conductivity equation, see Equation 19

B = intercept ceofficient in EDDY equation, see Equation 18

C_p = constant pressure specific heat

D = inside tank diameter

EDDY = dimensionless eddy conductivity factor, EDDY = $(\alpha + \varepsilon)/\alpha$

E_{INLET} = inlet value of dimensionless eddy conductivity factor

FLOW = dimensionless flow parameter, FLOW=$V\Delta t/\Delta x$

Fo = Fourier number, Fo=$\alpha\Delta t/\Delta x^2$

g = acceleration of gravity

ISLAB = location at slab I, see Equation 18

k = thermal conductivity

L = effective length between inlet and outlet

NSLAB = total number of slabs in the tank, see Equation 18

Re = Reynolds number, Re= VD/ν_{avg}

Ri = Densimetric Richardson number, Ri= $(\Delta\rho gL)/(\rho_{avg}V^2)$

t = time

T = temperature

V = velocity inside the tank

x = vertical direction in the tank

Greek Symbols

α = thermal diffusivity, $\alpha = k/\rho C_p$

$\Delta\rho$ = density difference between initial and inlet temperatures

Δx = incremental tank height

Δt = incremental time step

ΔT = temperature difference between initial and inlet

ε = eddy conductivity factor

ρ = density

ν = kinematic viscosity

Subscripts

avg = average property between inlet and initial

n = north of the point of interest

0 = initial property

p = point of interest

s = south of the point of interest

Superscript

' = value at new time level

REFERENCES

Abdoly, M. A. 1981. "Thermal stratification in storage tanks." Ph.D. dissertation, University of Texas at Dallas.

Cabelli, A. 1977. "Storage tanks - A numerical experiment." Solar Energy, 19, pp. 45-54.

Chow, C-Y. 1983. An introduction to computational fluid mechanics. pp. 331-336. Boulder, Colorado: Seminole Publishing Company.

Cole, R. L., and Bellinger, F. O. 1982. "Natural thermal stratification in tanks, Phase 1, final report." ANL 82-5.

Han, S. M., and Wu, S. T. 1978. "Computer simulation of a solar energy system with an entrainment energy storage tank model." Proceedings of the Third Southeastern Conference on Application of Solar Energy, Huntsville, Alabama.

Lavan, Z., and Thompson, J. 1977. "Experimental study of thermally stratified hot water storage tanks." Solar Energy 19, pp. 519-524.

Oppel, F. J. 1985. "Computer simulation for stratified thermal storage." M.S. thesis, Oklahoma State University.

Oppel, F. J.; Ghajar, A. J., and Moretti, P.M. 1986. "Computer simulation of stratified heat storage." Applied Energy 23, pp.205-224.

Sha, W. T., and Lin, E. I. H. 1978. "Three-dimensional mathematical model of flow stratification in thermocline storage tanks." Proceedings of the 3rd Southeastern Conference on Solar Energy, pp. 185-201.

Sharp, M. K. 1978. "Thermal stratification in liquid sensible heat storage." M.S. thesis, Colorado State University.

ACKNOWLEDGMENTS

This work was sponsored by the University Center for Energy Research (UCER) at Oklahoma State University.

TABLE 1

Computer Nomenclature

A	--	Area of the tank
AMIX	--	Nondimensional mixing constant, $(\alpha + \varepsilon)\ \Delta t/\Delta x^2$
ALPHA	--	Thermal diffusivity, $k/\rho C_p$
DELT	--	Time interval in the program, Δt
DELX	--	Distance between slabs in the tank, Δx
EDDY	--	Thermal eddy conductivity factor, $(\alpha + \varepsilon)/\alpha$
EMAX	--	Maximum eddy conductivity factor
FLOW	--	Nondimensional flow constant, $V\ \Delta t/\Delta x$
H	--	Height in the tank

(TABLE 1 continued)

NSLAB	--	Number of slabs in the tank
QMAX	--	Maximum flow rate of incoming flow
T	--	Temperature
TIN	--	Temperature of incoming flow
TO	--	Initial temperature in the tank
VEL	--	Velocity of water through the tank
VMAX	--	Maximum velocity of water through the tank

TABLE 2

Computer Input For Simulation (Sharp 1978)

Tank Specifications	**Fluid Properties**
H = 6.34 ft	TIN = 102 F
D = 3.8 ft	TO = 69 F
A = 11.34 ft^2	ρ = 62.4 lbm/ft^3
NSLAB = 20	k = 0.355 Btu/h·F·ft
DELX = 0.317 ft	C_p = 0.998 Btu/lbm·F
Insulated Tank	α = 0.0057 ft^2/h
Inlet Manifold Designed by (Sharp 1978)	QMAX = 0.84 ft^3/min
	VMAX = 7.44 x 10^{-2} ft/min
Stability Criterion	**Nondimensional Parameters based on DELX, VMAX**
FLOW: DELT $\leq$ 4.28 min	Pick DELT = 3.0 min
	FLOW = 0.70
	Fourier No. = 2.846 x 10^{-3}

TABLE 3

Simulation Results of Experimental Data of (Sharp 1978)

Case		Eddy Conductivity Factor Used	Allowable Range of Eddy Conductivity
Laminar Uniform (Curve 1, Fig. 4)		1	-
Turbulent Uniform (Curve 1, Fig. 4)		20	15-25
Turbulent Varying (Curve 1, Fig. 4)	(1)	25*	-
	(2)	15	
	(3)	5	
	(4)	1	
Laminar Uniform (Curve 2, Fig. 4)		1	-
Turbulent Uniform (Curve 2, Fig. 4)		10	5-15
Turbulent Varying (Curve 2, Fig. 4)	(1)	25*	-
	(2)	15	
	(3)	5	
	(4)	1	

* Eddy conductivity factors used in the four regions of the tank (turbulent varying case) where, 1 refers to the region next to the inlet and 4 refers to the region near the exit of the tank.

TABLE 4

Simulation Results of Experimental Data (Abdoly 1981) for the Decreasing Hyperbolic Function

Inlet Eddy Conductivity Factor	Inlet Temperature F	Initial Temperature F	Volumetric Flow Rate gpm	Reynolds Number	Richardson Number
1000	72	202	2	1000	9.03×10^4
800	68.5	202	1.09	529	3.07×10^5
500	67.5	201.5	0.55	263	1.20×10^6
1000	66	203	2	946	9.29×10^4
900	70	194	1.28	616	2.03×10^5

TABLE 5

Simulation Results of OSU Experimental Data for the Decreasing Hyperbolic Function

Inlet Eddy Conductivity Factor	Inlet Temperature F	Initial Temperature F	Volumetric Flow Rate gpm	Reynolds Number	Richardson Number
20	61	99	0.83	250	1.10×10^5
10	61	124	0.83	280	2.26×10^5
5	61	164	0.80	280	5.07×10^5
200	61	99	1.84	570	2.22×10^4
100	61	124	1.83	610	4.66×10^4
50	61	164	1.76	640	1.04×10^5
700	61	99	3.38	1040	6.6×10^3
500	61	124	3.40	1140	1.35×10^4
200	61	164	3.38	1220	2.8×10^4

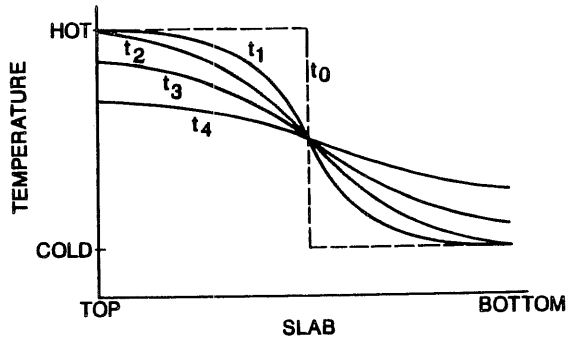

Figure 1. Temperature profile in tank for theoretical conduction-only case as time increases

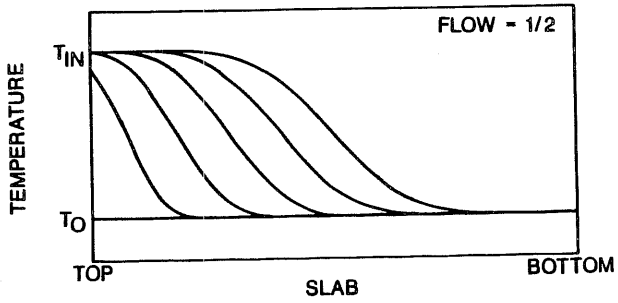

Figure 3. Temperature profile in tank for numerical convection-only (FLOW = 1/2) case as time increases

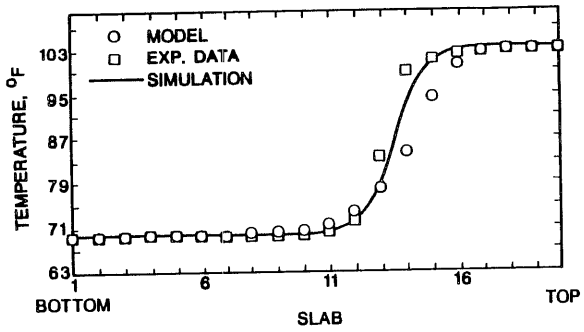

Figure 5. Comparison of storage tank temperature profiles for turbulent uniform case of curve 1 in Figure 4

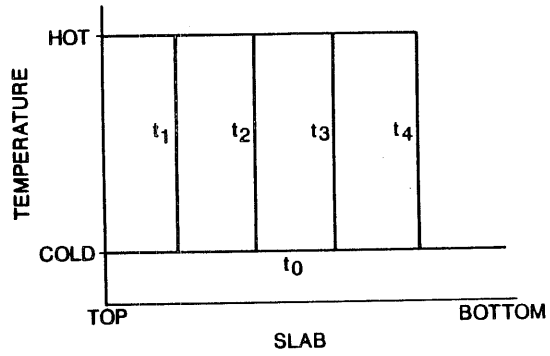

Figure 2. Temperature profile in tank for theoretical convection-only case as time increases

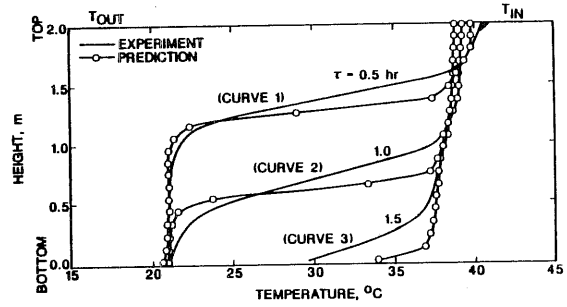

Figure 4. Prototype manifold, charging 6 gpm, taken from Sharp (1978)

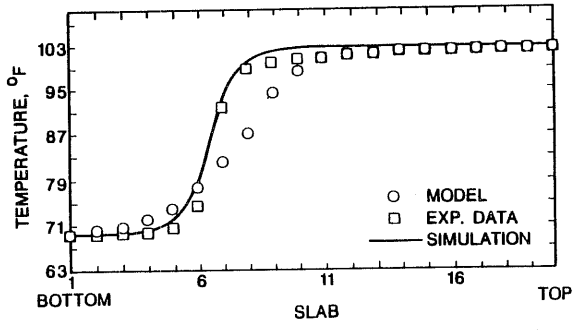

Figure 6. Comparison of storage tank temperature profiles for turbulent uniform case of curve 2 in Figure 4

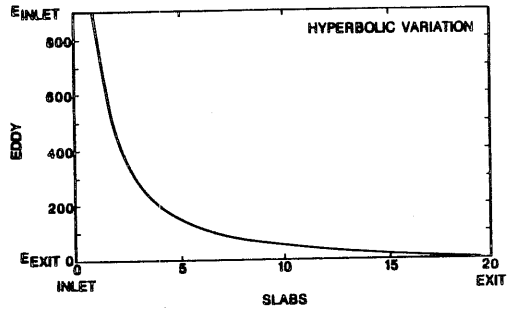

Figure 7. Eddy conductivity variation inside tank using a decreasing hyperbolic function for experimental data of Abdoly (1981)

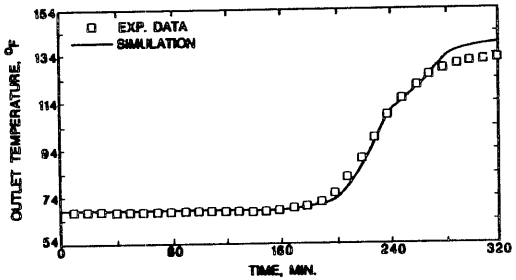

Figure 9. Simulation of experimental data of Cole and Bellinger (1982) for 0.75 l/min and 40°C ΔT using the hyperbolic function with the side-inlet-outlet design

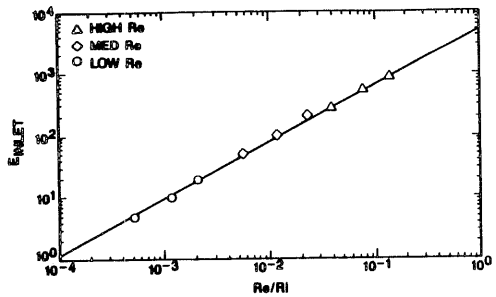

Figure 11. Inlet eddy conductivity vs. Reynolds number over Richardson number for OSU experimental data

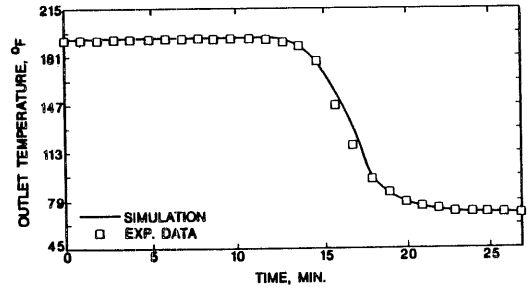

Figure 8. Simulation of experimental data of Abdoly (1981) for 1.28 gpm and 124 F using the hyperbolic function

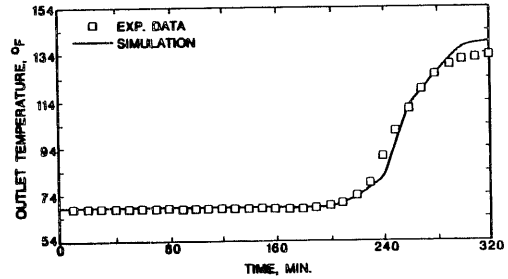

Figure 10. Simulation of experimental data of Cole and Bellinger (1982) for 0.75 l/min and 40°C ΔT using the hyperbolic function with the dual radial diffuser design

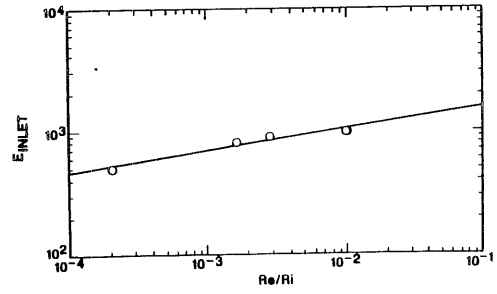

Figure 12. Inlet eddy conductivity vs. Reynolds number over Richardson number for experimental data of Abdoly (1981)